Anion vacancies as a source of persistent photoconductivity in II-VI and chalcopyrite semiconductors

Stephan Lany and Alex Zunger
National Renewable Energy Laboratory, Golden, Colorado 80401, USA
(Received 13 January 2005; revised manuscript received 12 April 2005; published 18 July 2005)

II. BASIC PHYSICS OF σ-TYPE AND π-TYPE DEFECT BEHAVIOR

The distinction between these two types of behaviors can be appreciated from simple two-level models in which the impure system is described via the interaction between an ideal (unrelaxed) vacancy (vac) state $\varepsilon_{\rm vac}^{\lambda,\gamma}$ in the pure host crystal and the orbitals $\varepsilon_{\rm I}^{\lambda,\gamma}$ of the isolated impurity (I) atom (Fig. 1).[3,25] Here, we consider only the dilute limit, where no interaction between impurity states exists. The vacancy of the pure host crystal can occur on either sublattice λ (i.e., λ=cation or λ=anion). Different vacancy levels can be constructed from the dangling bond hybrids of the neighboring host atoms, according to the irreducible representations γ of the corresponding λ site symmetry (e.g., $\gamma=a_1$ or $\gamma=t_2$ in the $T_{\rm d}$ point-group symmetry of the zinc-blende structure). We define $\varepsilon_{\rm vac}^{\lambda,\gamma}$ in Fig. 1 as the energy of the λ-site vacancy state with symmetry γ. Similarly, the isolated impurity atom on site λ has symmetry-adapted orbitals with energy $\varepsilon_{\rm I}^{\lambda,\gamma}$. The two unperturbed states $\varepsilon_{\rm vac}^{\lambda,\gamma}$ and $\varepsilon_{\rm I}^{\lambda,\gamma}$ are shown in Fig. 1 as dotted lines, representing varying impurities in a fixed host system.

Vacancy and impurity states of the same symmetry γ interact and repel each other, creating bonding and antibonding states (red solid lines in Fig. 1), as a function of the perturbation strength $\Delta V=\varepsilon_{\rm I}^{\lambda,\gamma}-\varepsilon_{\rm H}^{\lambda,\gamma}$, measured by the difference of atomic orbital energies between the impurity (I) atom and the host (H) atom it replaces.[25] As one expects, for extremal values of ΔV the energy of the DLS state saturates at the value of the host vacancy level. Indeed, when one regards the vacancy itself as the impurity, the energies $\varepsilon_{\rm vac}^{\lambda,\gamma}$ of the vacancy states are not altered by interaction with an impurity state $\varepsilon_{\rm I}^{\lambda,\gamma}$. As discussed below, the energies of the vacancy states can depend strongly on atomic relaxation, however.

In order to illustrate the range of physical behaviors that is implied with the α vs β behavior, we now add in Fig. 1 schematically (for the specific case λ=anion and $\gamma=a_1$) the position of the host band edges (blue horizontal solid lines), and integrate in the figu-7uln theathd2rbit(he)8-80TD85

dispersive impurity band[4,9] forms already at rather low concentrations, leading to a Moss-Burstein shift to higher energies if the PHS is occupied. For example, Astala and Bristowe,[27] as well as Buban and co-workers[28] calculated V_O^0 in $SrTiO_3$ and observed strong changes in total energy and atomic relaxation with increasing cell size (up to 320 atoms).

respect to the anion-s like $\Gamma_{1\nu}$ state. Thus E_V in Eq. (1) is corrected by $\Delta E_V = -0.77$, -0.34 -0.28, and -0.20 eV in ZnO, ZnS, ZnSe, and ZnTe, respectively, and by $\Delta E_V = -0.37$ eV in $CuGaSe_2$ and $CuInSe_2$. The amount of correction in the VBM is consistent, e.g., with the *GW* calculations for ZnO.[46] Still, the LDA+U band gaps, e.g., 1.53 eV in ZnO and ~ 0 eV in $CuInSe_2$, are much smaller than the experimental gaps [3.37 eV in ZnO (Ref. 47) and 1.04 eV in $CuInSe_2$ (Ref. 48)]. The remaining discrepancy is accommodated by shifting CBM upwards (by ΔE_C). In practice, we implement this correction by using the experimental band-gap energy E_g in Eq. (3) and for the allowed range $0 \leqslant \Delta E_F \leqslant E_g$ of ΔE_F in Eq. (1). We use the LDA+U scheme only to obtain the correction for the host band edges. The formation and transition energies presented in this work are obtained from Eqs. (1)–(4) using supercell total energies that are calculated in LDA. (We find, however, that the transition energies of V_{anion} calculated from LDA+U supercell energies differ only slightly.)

In the case of β-type defects that introduce electrons in the PHS, e.g., in the case of shallow donors, a correction $n\Delta E_C$ applies to ΔH when the PHS is occupied by n electrons. This is because the donor PHS can be assumed to shift along with the host CBM during band-gap correction. Similarly, a correction $-n\Delta E_V$ is applied to shallow acceptors when the acceptor state (valence-band-like PHS) is occupied by n holes. This is because the acceptor PHS can be assumed to shift along with the host VBM during band-gap correction. In the case of α-type defects, where the electrons or holes occupy the DLS rather than the host-band-like PHS, the latter two corrections are not applied, because it cannot be assumed that the localized DLS follows the band edges during band-gap correction. This procedure of letting the shallow levels (β-type PHS) follow the host band edges, but fixing the deep levels (α-type DLS) during band-gap correction differs from our previously employed schemes of band-gap correction, e.g., in Refs. 49 and 50. Indeed, the question of the extent of LDA-correction applied to α-type levels is a significant source of uncertainty in this and other [49,50] calculations. In order to assess more quantitatively how deep, α-type levels behave upon band-gap correction, *GW* calculations for such deep defects will be needed.

Several further corrections to the LDA calculated energies were applied, as discussed in more detail in another publication:[51] First, Moss-Burstein-like band-filling effects (cf. Sec. II) occur when electrons or holes occupy a perturbed-host state forming an impurity band in the supercell calculation. Such band-filling effects have also to be taken into account when, e.g., an unoccupied defect level drops below the VBM in the course of atomic relaxation, thus releasing holes to the valence band (cf. Sec. V). Second, the potential alignment between a charged defect calculation and the perfect host crystal is needed in order to correct for the effect of the compensating background charge. Third, the spurious interaction of periodic image charges is corrected to $O(L^{-5})$,[52] where L is the linear supercell dimension. The present scheme of treating finite supercell size effects and LDA errors has shown to yield good results for the optical transition energies of the color center in ZnS and ZnSe,[29] when compared with experimentally observed absorption energies.

IV. ANION VACANCIES IN ZnO AND OTHER II-VI

Having introduced in Sec. II the model of α- vs β-type behavior for the general case, where the impurity atomic orbitals interact with the states of the ideal vacancy, we now turn to the levels of the relaxed anion vacancy in ZnO and other II-VI compounds. As we have shown previously,[29] the energies of the vacancy orbitals (e.g., a_1 and t_2 in T_d symmetry) depend strongly on atomic relaxation of the cation neighbors. This is because these orbitals are constructed themselves from combinations of the dangling bond hybrids centered at each of the four cation neighbors, the totally symmetric a_1 state being bonding like. An inward relaxation increases the overlap between the dangling bond hybrids, thus lowering the energy of the a_1 state. Generally, the occupation

singly occupied DLS within the band gap, i.e., being α-type. The equilibrium Zn-Zn distance of V_O^+ is estimated[53] as $d_{\text{Zn-Zn}} \approx 3.2$ Å [Fig. 3(b)]. Due to the single occupancy of the DLS, the V_O^+ state is active in electron paramagnetic resonance (EPR), and is indeed observed in EPR experiments under illumination.[54,55] A second excitation $V_O^+ \rightarrow V_O^{2+} + e$ occurs at $\varepsilon_o(+/2+;e) \approx +2.4$ eV, producing the V_O^{2+} state with $d_{\text{Zn-Zn}} = 4.0$ Å [Fig. 3(b)]. Following this large outward relaxation, the DLS moves upward, becoming resonant inside the conduction band [Fig. 3(a), right-hand side]. Consequently, the photoexcited electrons occupy the lower energy PHS rather than the DLS, i.e., the V_O^{2+} vacancy assumes β-type behavior [Fig. 3(a), right-hand side]. The electrons in the PHS are now only shallowly bound through the screened Coulomb potential.

Figure 4(a) shows as a function of the Fermi energy E_F the formation energies of the light-induced metastable configuration of V_O^0 and V_O^+ (dashed lines), relative to the corresponding formation energies in the respective equilibrium stable configuration (solid lines).[56] The transition energies in the metastable β-type configuration [open circles in Fig. 4(a)] are close to the CBM,[57] so that this configuration is conductive. These shallow binding energies of the electrons in the PHS are also schematically indicated in Fig. 3(b) by the vertical displacement of the energy curves at $d_{\text{Zn-Zn}} = 4.0$ Å. The reaction path including both excitations in Fig. 3(b) leads to the light-induced transition

$$V_O^0 \rightarrow V_O$$

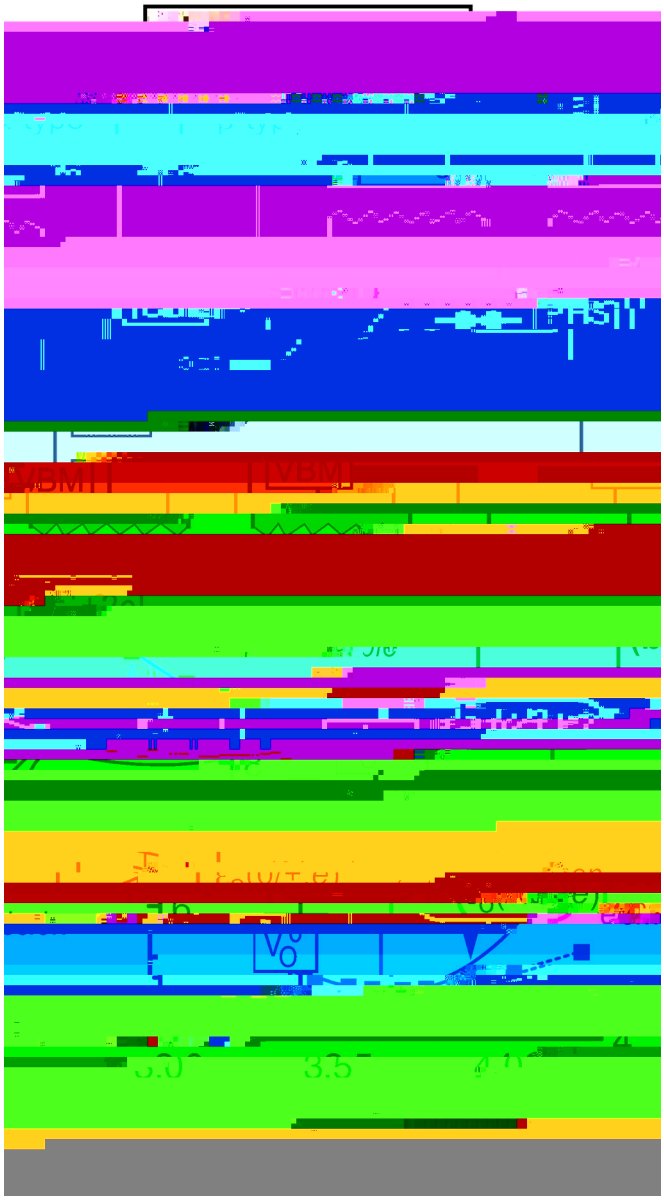

FIG. 3. (Color online) (a) Schematic energy diagram for V_O in ZnO, causing *n*-type PPC. Electrons that occupy the DLS or the PHS are depicted as solid circles.

$\varepsilon_o(0/+;e)$ transition in Fig. 3(b)]. Due to its positive charge, V_O^+ creates a hydrogenic-like PHS below the CBM, which can be populated by a conduction-band electron. The spin of the electron in the PHS can align either parallel ($S=1$) or antiparallel ($S=0$) with the spin of the electron in the deep a_1^1 state (DLS) of V_O^+. While the short-lived singlet ($S=0$) state does not give rise to any ODMR signal, the triplet ($S=1$) state is active in ODMR and has a rather long lifetime, because the radiative recombination of the electron from the PHS into the DLS involves a spin flip. This recombination causes the green emission at 2.45 eV, corresponding to the theoretical $\varepsilon_o(+/0;-e)\approx-2.1$ eV transition in Fig. 3(b).[61]

The observation of a $S=1$ state in the recent experiments using moderately *n*-type samples contrasts with the observation of a $S=1/2$ state in the classic EPR experiments,[54,55,62] where the samples were compensated either by additional Li

doping[55] or by high-energy electron irradiation,[54,62] which creates a variety of intrinsic defects. This behavior is readily understood in our model where the α-type V_O^+ forms the triplet state by binding a conduction-band electron in *n*-ZnO, but not in the compensated samples, where photoexcited electrons can recombine with acceptor states, or relax from the conduction band into other donor states.

Very recently, after completion of our calculations and submission of our paper, ODMR experiments in high-energy electron irradiated ZnO were reported.[63] *Before* the electron irradiation, the $S=1$ triplet was detected, similar to what was observed in Refs. 58 and 59. This required excitation above the energy threshold of 3.1 eV required for the $V_O^0 \rightarrow V_O^+ + e$ transition. *After* the electron irradiation, only the $S=1/2$ state was observed. This state was also produced by excitation far below the 3.1 eV absorption level, indicating that in the defect-rich irradiated samples, where electrons and holes can be created by sub-bandgap illumination, there exist other channels for the excitation of the paramagnetic V_O^+ state, such as, e.g., $V_O^0 + h \rightarrow V_O^+$. In fact, already the classic *F*-center experiments[62] showed, in addition to the 3.1 eV level, a broad absorption band in the EPR excitation spectrum with an onset around 1.6 eV and a maximum around 2.3 eV. In Ref. 63, the authors showed that the ODMR of the $S=1/2$ state of V_O^+ results from a spin-dependent electron capture process, where an electron is transferred from a shallow donor into the a_1^1 level of V_O^+, thus forming $V_O^0(a_1^2)$. They suggest two models that cannot be distinguished by their experiment: In the first, direct model, the photoluminescence used to detect the ODMR originates from the radiative electron capture itself. Taking into account the Stokes shift, this model places the $\varepsilon(+/0)$ level at $\sim E_V + 0.9$ eV. In the second, indirect model, the luminescence results from a subsequent hole capture of V_O^0. In this model, the $\varepsilon(+/0)$ would be at $\sim E_V + 2.5$ eV. Our numerical result $\varepsilon(+/0) = 0.94$ eV is in

of V_X (X=O, S, Se, and Te). The band edges are aligned according to the calculated[71,72] band offsets, taking also into account the present correction ΔE_V for the VBM (see Sec. III). According to our reaction path for the light-induced transition from α to β behavior (Fig. 3), two conditions have to be satisfied for the occurrence of PPC: (i) The neutral charge state V_X^0 must be the initial equilibrium stable state. This means that PPC can occur only when the Fermi level is above the $\varepsilon(2+/0)$ transition level. Since the calculated $\varepsilon(2+/0)$ level (blue line in Fig. 5) is located around mid-gap in all II-VI compounds, PPC can occur in n-type, but not in p-type material. (ii) V_X^{2+} must assume the conducting β-type behavior, i.e., the unoccupied a_1^0

=3.89 Å. In the latter situation, energy can be further lowered by constructing the DLS from only $N=2$ dangling bond orbitals, leading to the C_{2v} symmetry and a very close Zn-Zn

tively charged states V_{Se}^{-} and V_{Se}^{2-}. While the singly charged V_{Se}^{-} and V_{Se}^{+} are unstable due to negative-U behavior, the doubly charged V_{Se}^{2-} gives rise to a very deep *acceptor* state of V_{Se} which is actually close to the CBM, i.e., $\varepsilon(0/2-) = E_V + 0.97$ eV $= E$Se

sition $V_{Se}^{2+} \rightarrow V_{Se}^{0} + 2h$. The underlying mechanism for the metastability, i.e., the formation (V_{Se}^{0}) and breakup (V_{Se}^{2+}) of In-In bonds, is still operational in the vacancy complex, leading to *p*-type PPC by the analogous reaction

$$(V_{Se}\text{-}V_{Cu})^{+} \rightarrow (V_{Se}\text{-}V_{Cu})^{-} + 2h. \qquad (7)$$

In contrast to V_{Se}^{0}, the negatively charged vacancy complex on the right-hand side of the reaction (7) can bind one hole with the calculated activation energy $E_a = 0.27$ eV being in excellent agreement with the experimental hole trap depth 0.26 eV.[79] This energy corresponds to the $\varepsilon(0/-)$ acceptor level which is present *only* in the light-induced metastable configuration where the complex has the short-distance In-In bond. Here, the mechanism for *p*-type PPC requires that the positively charged complex [left-hand side of Eq. (7)] be the equilibrium ground state. The calculated $\varepsilon(+/-) = 0.31$ eV transition of the vacancy complex is much deeper in the gap than the analogous $\varepsilon(2+/0) = 0.02$ eV level of the isolated V_{Se}, so that the requirement of the initial $(V_{Se}\text{-}V_{Cu})^{+}$ state is fulfilled in *p*-$CuInSe_2$. Therefore, we suggest that the metastability observed in actual $Cu(In,Ga)Se_2$ experiments stems from the $(V_{Se}\text{-}V_{Cu})$ vacancy complex rather than from the

[24] D. L. Staebler and C. R. Wronski, Appl. Phys. Lett. **31**, 292 (1977).
[25] H. P. Hjalmarson, Ph.D. thesis, University of Illinois, 1979.
[26] Studying V_{Se}^{0} in ZnSe for supercells containing up to 128 atoms, we found that the total energy is converged within 0.02 eV for cells with 32 atoms and larger, despite the impurity bandwidth of ~0.8 eV for the 32 atom cell. The impurity band dispersion occurs mainly close to the Brillouin-zone center, and it causes a low-energy tail of the defect state with only little density of states, hardly affecting the total energy.
[27] R. K. Astala and P. D. Bristowe, Modell. Simul. Mater. Sci. Eng. **12**, 79 (2004).
[28] J. P. Buban, H. Iddir, and S. Ögüt, Phys. Rev. B **69**, 180102(R) (2004).
[29] S. Lany and A. Zunger, Phys. Rev. Lett. **93**, 156404 (2004).
[30] Y. J. Zhao, C. Persson, S. Lany, and A. Zunger, Appl. Phys. Lett. **85**, 5860 (2004); S. Lany, Y. J. Zhao, C. Persson, and A. Zunger, *ibid.* **86**, 042109 (2005).
[31] J. Ihm, A. Zunger, and M. L. Cohen, J. Phys. C **12**, 4409 (1979).
[32] (a) D. M. Ceperley and B. J. Alder, Phys. Rev. Lett. **45**, 566 (1980); (b) J. P. Perdew and A. Zunger, Phys. Rev. B **23**, 5048 (1981).
[33]

[71] S. H. Wei and A. Zunger, Appl. Phys. Lett. **72**, 2011 (1998).
[72] S. H. Wei and A. Zunger, J. Appl. Phys. **78**, 3846 (1995).
[73] S. Lany, H. Wolf, and Th. Wichert, Physica B **308-310**, 958 (2001).
[74] The choice of the host lattice constant affects somewhat the calculated energy differences: Using the (smaller) LDA lattice constant instead of the experimental one, we find $E[C_{2v}]-E[T_d] = +0.02$, -0.09, and -0.38 eV for ZnS, ZnSe, and ZnTe, respectively. However, using the GGA for the exchange-correlation potential and the respective (larger) GGA equilibrium lattice constant yields again a larger energy gain due to symmetry lowering and metal-metal dimer formation, e.g., $E[C_{2v}]-E[T_d] = -0.26$ eV for V_{Se} in ZnSe.
[75] D. J. Chadi, Mater. Sci. Semicond. Process. **6**, 231 (2003).
[76] S. M. Wasim, Sol. Cells **16**, 289 (1986).
[77] U. Rau and H. W. Schock, Appl. Phys. A: Mater. Sci. Process. **69**, 131 (1999).
[78] Recent theoretical studies (Ref. 30) indicate that *n*-type dopingChaeas.Cu-418